

SELF-TRAINABLE 3D-PRINTED PROSTHETIC HANDS

By

KYUNGHO NAM

Bachelor of Science in Electrical Engineering  
Oklahoma State University  
Stillwater, Oklahoma  
2015

Submitted to the Faculty of the  
Graduate College of the  
Oklahoma State University  
in partial fulfillment of  
the requirements for  
the Degree of  
DOCTOR OF PHILOSOPHY  
December, 2022

# SELF-TRAINABLE 3D-PRINTED PROSTHETIC HANDS

Dissertation Approved:

Christopher John Crick

---

Dissertation Adviser

Blayne E. Mayfield

---

Nohpill Park

---

Guoliang Fan

---

## ACKNOWLEDGEMENTS

I cannot express my gratitude enough to my academic advisor Dr. Christopher John Crick for his continued support and encouragement. I offer my sincere appreciation for the learning opportunities provided by him. At the end, glory and thanks to the God, the Almighty, for His helps throughout my research life to complete the research successfully.

---

Acknowledgements reflect the views of the author and are not endorsed by committee members or Oklahoma State University.

Name: KYUNGHO NAM

Date of Degree: DECEMBER, 2022

Title of Study: SELF-TRAINABLE 3D-PRINTED PROSTHETIC HANDS

Major Field: COMPUTER SCIENCE

Abstract:

3D printed prosthetics have narrowed the gap between the tens of thousands of dollars cost of traditional prosthetic designs and amputees' needs. However, the World Health Organization estimates that only 5-15% of people can receive adequate prosthesis services **WHO**. To resolve the lack of prosthesis supply and reduce cost issues (for both materials and maintenance), this paper provides an overview of a self-trainable user-customized system architecture for a 3D printed prosthetic hand to minimize the challenge of accessing and maintaining these supporting devices. In this paper, we develop and implement a customized behavior system that can generate any gesture that users desire. The architecture provides upper limb amputees with self-trainable software and can improve their prosthetic performance at almost no financial cost. All kinds of unique gestures that users want are trainable with the RBF network using 3 channel EMG sensor signals with a 94% average success rate. This result demonstrates that applying user-customized training to the behavior of a prosthetic hand can satisfy individual user requirements in real-life activities with high performance.

# CONTENTS

Chapter	Page
I INTRODUCTION . . . . .	1
II LITERATURE REVIEW . . . . .	3
2.1 3D-printed prostheses . . . . .	3
2.2 EMG-based human robot interaction . . . . .	3
2.3 EEG-based human robot interaction . . . . .	4
III CONTROL SYSTEM ARCHITECTURE COMPONENTS . . . . .	6
3.1 3D-printed prosthetic hand . . . . .	6
3.2 Electrical biosignal sensors . . . . .	7
3.2.1 Electromyography sensors . . . . .	7
3.2.2 EMG signal processing . . . . .	8
3.2.3 Electroencephalogram sensors . . . . .	9
3.2.4 EEG signal processing . . . . .	9
3.3 Self-training user-customized control software . . . . .	9
IV PRELIMINARY EXPERIMENTATION AND RESULTS . . . . .	12
V CONCLUSION . . . . .	21
5.1 Self-trainable 3D-printed prosthetic hands . . . . .	21
5.2 Milestone . . . . .	21

## LIST OF TABLES

Table	Page
4.1 Experiments with different actions . . . . .	15
4.2 Average recognition success rates of the trained RBF network, linear SVM network, and MLP network . . . . .	16

## LIST OF FIGURES

Figure	Page
3.1 3D-printed prosthetic hand . . . . .	7
3.2 The layout of the MyoWare Muscle Sensor (AT-04-001) . . . . .	8
3.3 An example of EMG signals processing . . . . .	8
3.4 Radial basis function model . . . . .	11
4.1 Procedures of the system architecture . . . . .	13
4.2 User's unique gesture (Pinky Swear) training with 3 EMG sensors . . . . .	14
4.3 Collected 3-channel EMG sensor values for each different action . . . . .	18
4.4 Confusion matrix represents the accuracy per user action label . . . . .	19
4.5 Average recognition success rates of the trained RBF network, linear SVM network, and MLP network under different levels of noise inputs . . . . .	20
5.1 Milestone . . . . .	22

## CHAPTER I

### INTRODUCTION

Article 25 of the Convention on the Rights of Persons with Disabilities, adopted by the General Assembly of the United Nations, establishes the right to receive the highest feasible standard of health care without discrimination on the basis of disability from State Parties **UN**. Concerning amputees, the provision of affordable and high-quality prosthetic aids is a human rights argument, one that governments must support. Nevertheless, World Health Organisation figures show that only 5-15% of the population in need is able to access prosthetic and orthotic appliances in today's world **WHO**. The difficulty of accessing such devices is greater in low- and middle-income countries. In such areas, charities, often staffed by people who are not trained professionals, often provide prosthetic and orthotic services, leading to compromised services and poor quality and fit. In addition, without adequate provision for maintenance, people are often restricted in their quality of life, excluded from participating in society, and locked into poverty and isolation **WHO**. Most amputees who have any kind of prosthetic hand at all are only able to obtain a cosmetic hand, which affords a realistic appearance **3D4** but provides little functionality for grasping objects or anything else.

One of the main issues for useful prostheses is cost. The total mean life cost for an amputee is reported to be \$509,275 **cost\_1**. The weighted average prosthesis price is \$10,232, and total costs for the prosthesis after the second year are \$181,500 **cost**. The



annual maintenance costs for a functional prosthesis are expected to be 20% of the initial prosthesis' price, for a total of \$83,490 after the second year.

Most studies in the field of prosthetics have focused on reducing acquisition costs and improving performance. However, maintenance service for prostheses has not been nearly as heavily studied. Amputees with prostheses certainly require such ongoing service, especially as new situations arise. For instance, child users grow up and need larger-sized prostheses, and old prosthetics suffer decreased performance. To address the necessity of excellent quality maintenance service and the lack of low-cost, high-performing prostheses, this paper introduces an architecture that can be self-trainable and user-customized, based on a very low-cost 3D-printed prosthetic hand. This architecture provides self-trainable software to the user, which can increase the prosthetic hand's performance at a very low financial cost. A small amount of time invested in training the user's prosthesis returns high accuracy in its performance with repetitive behavior.

## CHAPTER II

### LITERATURE REVIEW

#### 2.1 3D-printed prostheses

Currently, only 5-15% of people who need them have access to prostheses **WHO**, so much effort and research is going into expanding the availability of low-cost prosthetics. Several recent works **3D43D2** aimed to build a low-cost robotic prosthetic arm using 3D printing technology with capable and comfortable design. 3D printing technology suggests a new path to satisfying amputees' financial needs and various physical conditions, while also enabling departures from the prosthesis's standard size for children or veterans with upper limb loss. **3D3** For similar reasons, in order to minimize the cost of supplying the prosthesis to more people, a 3D-printed hand was chosen as the basic structure for this study.

#### 2.2 EMG-based human robot interaction

Electromyography (EMG) **review**; **EMG** is one of several biological signals produced by the human body which can be used to predict motor intentions, in addition to such signals as electrical ultrasound (EOG) **EOG**, electrical ECG **ECOG**, EEG **EEG\_1**, and brainwaves (MEG) **MEG**. Likewise, many different sensors have been used to read users'

intentions to control their prostheses **MMG**. In particular, EMG sensors are available that are both highly accurate and low cost, and can be used to control diverse devices. The most attractive aspect of an EMG sensor is that it is a hands-free sensor that does not require invasive surgery. EMG sensors **controlEMG** have been used to control a mouse **mouse**, a mobile RC car **RCcar**, and even to assemble a Rubik's cube **rubikcube**.

### 2.3 EEG-based human robot interaction

Another non-invasive control techniques that translate imagined hand movements into motor signals use electroencephalograms (EEGs) **EEG** as Brain-Machine Interfaces. An EEG-based study work [??] developed and validated a neuro-based method for objectively verifying robot behavior in HRI, and proposed to detect improper / unexpected / erroneous robot behavior using the electroencephalogram (EEG) of a human interaction partner. EEG-based brain-controlled mobile robots can be useful tools for severely disabled persons in their daily lives, particularly when it comes to assisting them in moving voluntarily. **EEG** This EEG human-robot interaction technique has already been successful in detecting and classifying simple hand motions. [??]

Our research relies on a hand prototype **3D1** which emulates the structure of a human hand using 5 servo motors and electromyography (EMG) sensors to detect the electrical potential when muscle contraction appears.

The novel problem we consider is customizing a cheaply-produced 3D-printed prosthetic device for each diverse user. A perfectly fitting prosthesis with high performance for all the different individuals is impracticable. Most of the research in the field of prosthetic hands focused only on reducing cost or improving performance, while prosthesis maintenance services have not been as intensely studied. Adequate after-care maintenance services for amputees who use the prosthesis are extremely important. We have developed an

architecture that allows users to train their devices to have high-performance and creative idiosyncratic behaviors tailored exactly to their individual use cases.

## CHAPTER III

### CONTROL SYSTEM ARCHITECTURE COMPONENTS

In this section, we provide a detailed description of the individual control system components of this architecture.

#### 3.1 3D-printed prosthetic hand

Many open-source 3D-printable prosthetic hands are available. All of our prosthesis parts are defined in stereolithography (STL) files **STL** with different designs that can be modified for the best-fitting model for each different user. Armed with those STL files, the 3D printer can generate a prosthetic hand with diverse sizes for different people who need it. For the experiments, an open-source design was adopted and printed with a 3D printer, which is easily modified in the future for each user's needs.

In our prosthesis prototype, five MG996R servo motors with a maximum stall torque of 11 kgf-cm powered by 6V are used as actuators, one for each finger **3D1**. The motors are controlled by an Arduino Mega Atmel 8-bit AVR microcontroller. When the EMG sensors detect a muscle contraction, the microcontroller controls individual servo motors to control individual fingers in real-time through the decision-making process. The printed 3D prosthetic hand is shown in Fig. 5.1.



**Figure 3.1** 3D-printed prosthetic hand

### 3.2 Electrical biosignal sensors

#### 3.2.1 Electromyography sensors

To detect and measure the electrical activity produced by muscle contraction, the electrodiagnostic technique is considered as an input for the decision-making process. The MyoWare Muscle Sensor is used, which is designed for microcontroller applications **myo** with the dimension of 52.3x20.7mm. It needs a voltage power between 2.9-5.7 V with a maximum current of 14mA. As shown in Fig. 3.2, the sensor can measure the muscle's electrical potential with three electrodes when the sensor board is placed at the skin above the targeted muscle.

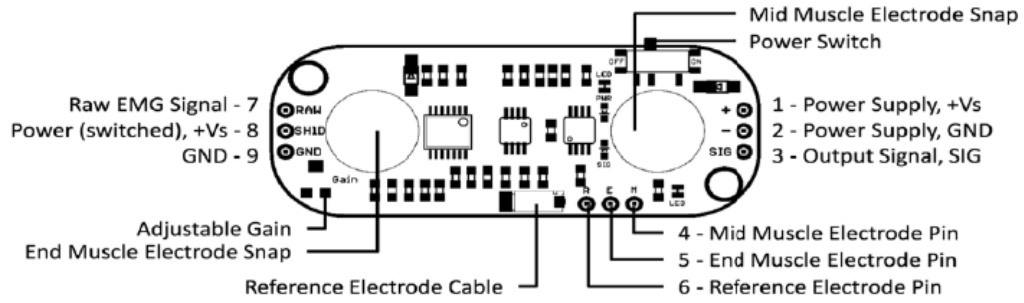


**Figure 3.2** The layout of the MyoWare Muscle Sensor (AT-04-001)

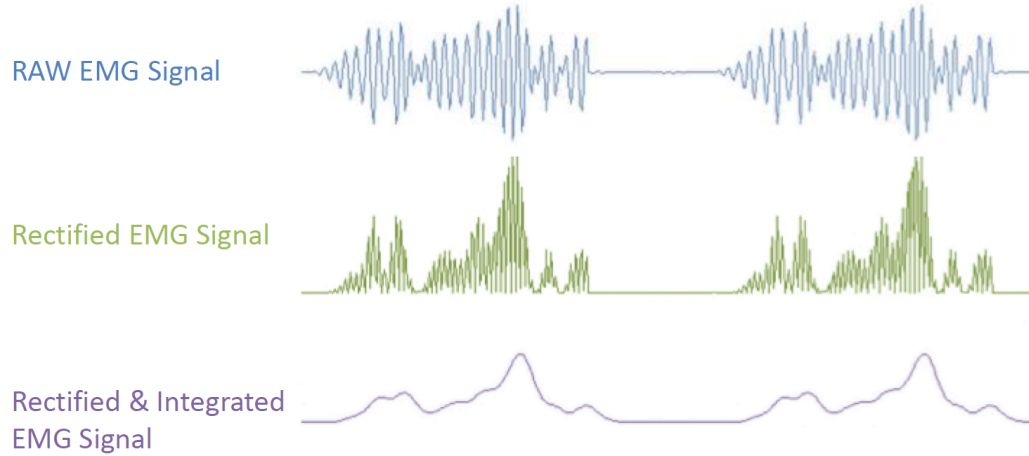


**Figure 3.3** An example of EMG signals processing

### 3.2.2 EMG signal processing

The MyoWare Sensor can detect envelope EMG and raw EMG with the voltage signal difference between the central muscle electrode and the reference electrode. The sensor generates the envelope signal, which is amplified, rectified, and integrated within the sensor transducer, as shown in Fig. 3.3. The signal amplitudes are translated through the microcontroller's analog-to-digital converter (ADC), and are then utilized as features to select human behaviors at the decision-making process.

### 3.2.3 Electroencephalogram sensors

Electrodes placed on your scalp detect tiny electrical charges that result from the activity of your brain cells to identify and measure the electrical activity produced by irregularities in your brain signals or electrical activity of your brain. The electrodiagnostic approach is used as a source of information for decision-making. The Muse S brain sensing headband is used, which is designed for a multi-sensor brain-computer interface headband that can give you real-time feedback on your brain waves.

### 3.2.4 EEG signal processing

The Muse S can detect signals from TP9, AF7, AF8, TP10 in the international standard EEG placement system. According to the technical manual [???], Muse S receives a raw signal ranging from 0 to 1682 microvolts (V), which can represent the raw data of each sensor. Fast Fourier Transform (FFT) of raw data is used to generate discrete frequency values on the log scale. The frequency bands of the brain waves can be determined using a spectrum of discrete frequency data: Gamma (30-44 Hz), Beta (13-30 Hz), Alpha (7.5-13 Hz), Theta (4-8 Hz), and Delta (1-4 Hz). Based on the Power Spectrum Density (PSD) log of EEG data for each channel, this absolute band power is utilized as a function of selecting human behavior in the decision-making process.

## 3.3 Self-training user-customized control software

In our software designed to train the user's prosthetic hand, all the magnitude of the envelope signals, generated by 3 channel EMG sensor signals, were transferred to the Arduino platform. The microcontroller can read and record all the sensor data as a user history to train each behavior into the machine. In the trained device, these three matrix values contain sensor values (0-1000) as inputs, which are used to produce prosthetic hand



behavior decision-making in real-time. The training function procedure and the actual operation function procedure are presented in Algorithm 3.1.

---

**Algorithm 3.1** System architecture

---

```

1: procedure TRAINING
2:    $y.append(CustomGesture)$  ▷ custom new gesture
3:   for  $i = y_0$  to  $y_{max}$  do
4:     for  $j = 0:T$  do
5:        $X_j^i \leftarrow readSensors()$ 
6:     end for
7:   end for
8:    $clf.fit(X, y)$ 
9: end procedure
10: procedure MOVEMENTS
11:   while  $r \neq 0$  do
12:      $Gesture = predict(readSensors())$ 
13:      $MotorController(Gesture, servoMotors())$ 
14:   end while
15: end procedure

```

---

To train the model, a user's custom gesture is appended (as many as desired). Each  $y$  contains each custom gesture per  $T$  iterations, and each sensor's value is recorded in  $X$  for the classification. The motor outputs provided to move each finger by motor controller depend on the prediction for the user's specific gesture.

A support vector machine (SVM) **ML1ML2** supervised learning methods, is applied to the prosthetic hand's behavior classification, with a radial basis function (RBF) kernel. The radial basic function network has the advantage of solid tolerance to input noise and is well suited for designing flexible control systems **RBFAdv**. This gesture classification uses multiple EMG sensors as input matrix  $X$ , and the output matrix  $y$  consists of each different individual intended gesture.

The equation (3.1) defines the radial basis function kernel for two different inputs  $X$  and  $X'$ , designated as feature vectors, which is the factor to predict purposing action with

trainable high-performance accuracy.

$$K(X, X') = \exp\left(-\frac{\|X - X'\|^2}{2\sigma^2}\right) \quad (3.1)$$

The squared Euclidean distance between the two feature vectors is shown in  $\|X - X'\|^2$ .

The  $\sigma$  worked as a parameter condition.

The artificial neural network interpretation of SVMs using radial basis function kernel to train the prosthesis is demonstrated in Fig. 3.4.

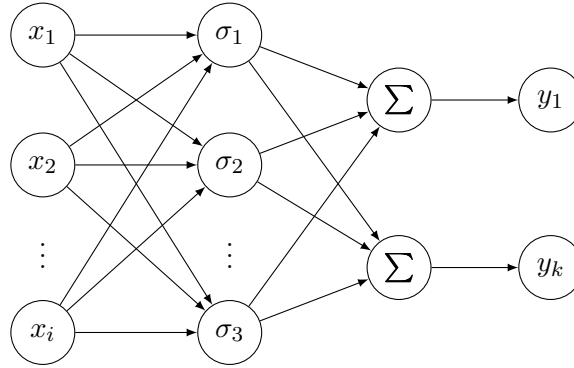


**Figure 3.4** Radial basis function model

The support vector classification implementation is tuned with regularization parameter  $C = 2.5$ , and the kernel coefficient for RBF  $\gamma = 0.01$  as the best fit.

## CHAPTER IV

### PRELIMINARY EXPERIMENTATION AND RESULTS

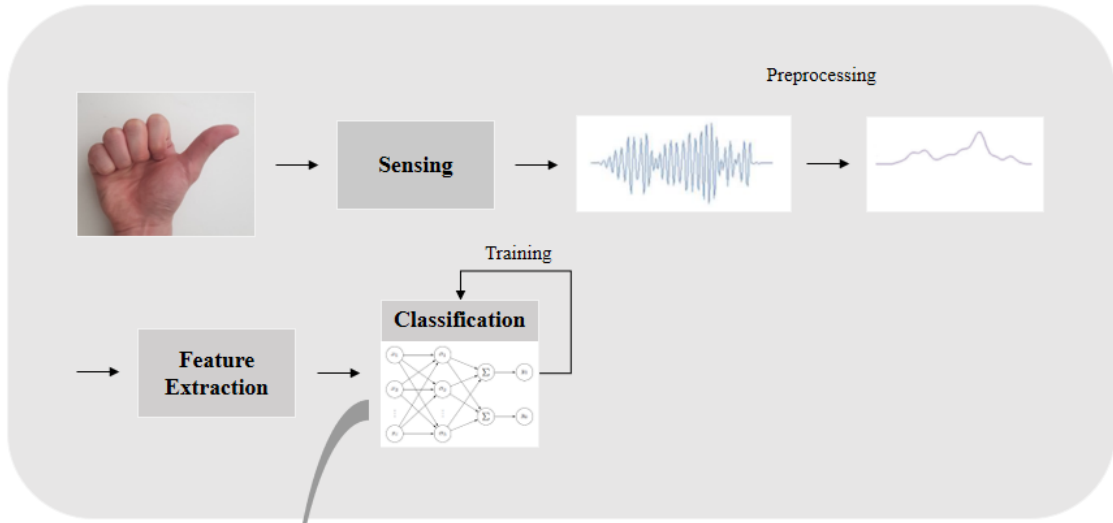
In order to evaluate the performance of the architecture, this system is designed in two different modes, which is depicted in Fig 4.1.

In training mode, when the test subject group performs each different action, 3 different EMG sensors read the subjects' muscle contraction. The raw EMG sensor signals are rectified in real-time as feature values for classification. In real-life mode, the test subjects perform the same actions to practically actuate the 3D printed prosthetic hand. In this mode, sensing, preprocessing, and feature extraction are processed, the same as in training mode. However, this real-life mode predicts the subjects' actions using a trained classification model to generate classification results. This classification result is transferred to the motor controller to control each motor assigned with each finger.

The experiments were conducted with  $n = 7$  test subjects containing 5 males and 2 females in their 20s and 30s. Each subject in the experiment was instructed to attach three EMG muscle sensors to their muscles, shown in Fig 4.2. The group was not composed of amputees, though such individuals will be recruited for subsequent experiments. The placement of the three EMG sensor devices on the forearm was chosen to accommodate amputees.

The EMG muscle sensors are attached to the area of the flexor digitorum superficialis,

**- Training Mode**



**- Real Life Mode**

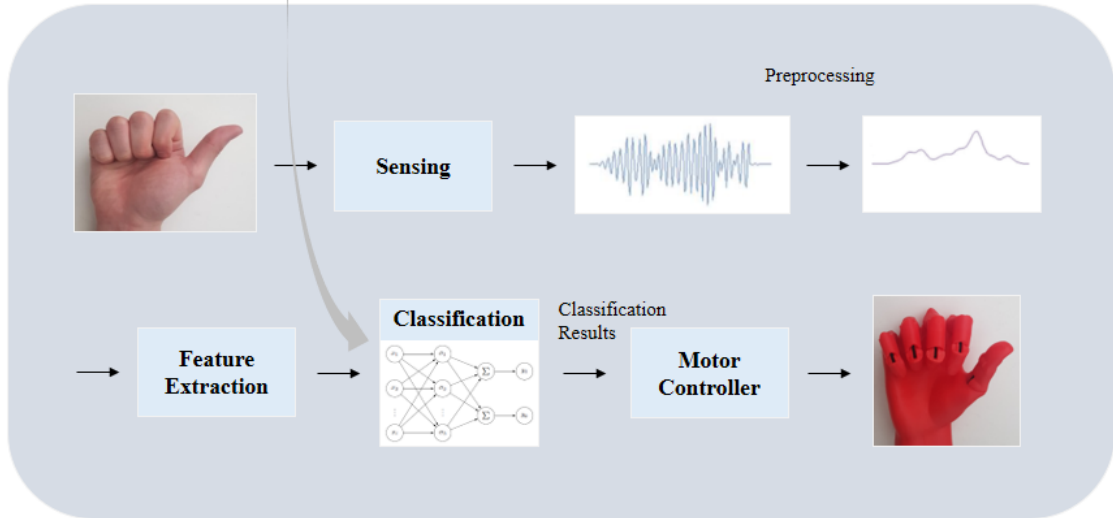


**Figure 4.1** Procedures of the system architecture

which is an extrinsic flexor muscle that actuates four fingers with the interphalangeal joints, the flexor digitorum profundus, which is the muscle that can bend the fingers to grip, and the flexor pollicis longus, which actuates thumbs, particularly for writing and

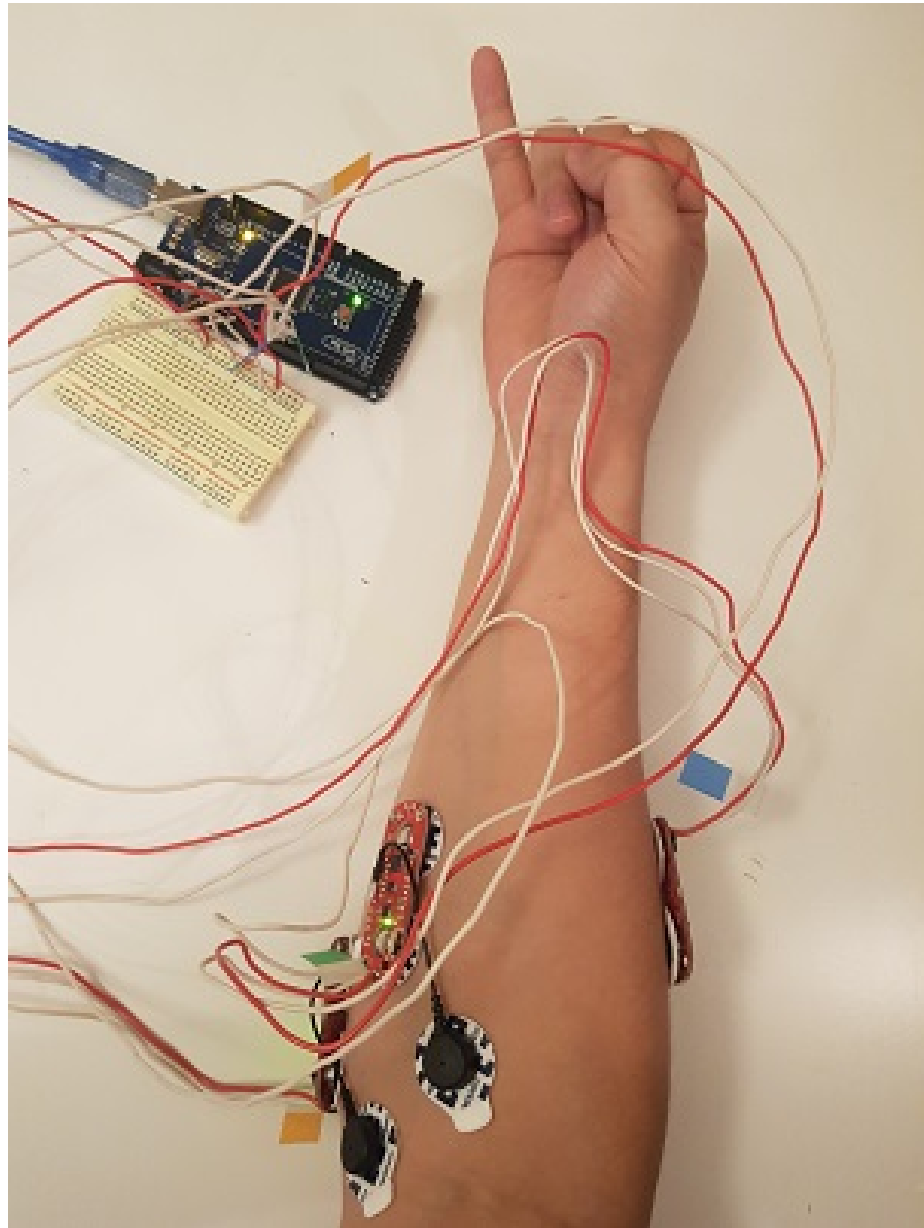


**Figure 4.2** User's unique gesture (Pinky Swear) training with 3 EMG sensors

painting.

To train various gestures into the prosthetic hand, a trial of using the prosthetic hand with 3 EMG MyoWare Muscle Sensors was performed. The subject tried to contract his muscles

to perform his intended hand behavior. 200 samples of EMG sensor data were recorded during each action.

To testify to the decision-making algorithm’s practicality, the experiment routine is conducted for numerous behaviors, with the EMG signals used to classify each different hand movement.

Each gesture is repeated, and simultaneously the 200 EMG muscle sensor values are recorded when the user performs the motion as shown in Table 1.

**Table 4.1** Experiments with different actions

User behavior	Each iteration
Hand Relax	200
Clenching fist	200
Open hand	200
Thumbs up	200
Pointing somewhere	200
OK sign	200
Ball grip	200
Pencil grip	200
Smartphone grip	200
User’s unique gesture (whatever the subject wants)	200

Any user’s customized unique gestures are recorded in the ‘User’s unique gesture (whatever the subject wants),’ which can potentially offer customization for each different user.

Fig. 4.3 illustrates two representative histories of each EMG sensor variables’ clusters. Each scatter plot color represents a different labeled gesture. Each axis of the graph shows the actual sensor variable boundary between 0 to 1000 amplitude, measured by 3 different MyoWare Muscle Sensors.

The evaluation results of the model are illustrated with a confusion matrix as shown in Fig. 4.4, which shows the accuracy per user action label. Each column corresponds to the

**Table 4.2** Average recognition success rates of the trained RBF network, linear SVM network, and MLP network

	<i>RBF</i>		<i>LinearSVM</i>		<i>MLP</i>		
	<i>Subject</i>	<i>Training set</i>	<i>Test set</i>	<i>Training set</i>	<i>Test set</i>	<i>Training set</i>	<i>Test set</i>
<i>without noise</i> = 1		95.69%	95.50%	88.25%	89.25%	90.50%	89.50%
	2	92.00%	90.00%	90.44%	89.50%	84.50%	84.50%
	3	97.19%	89.25%	89.19%	86.50%	87.44%	83.00%
<i>with noise</i> = 4		92.06%	80.75%	79.25%	77.00%	68.38%	67.25%
	5	82.25%	80.50%	77.00%	73.50%	70.25%	68.50%
	6	88.44%	75.75%	68.94%	71.25%	65.06%	69.75%
	7	88.56%	83.25%	67.69%	67.50%	64.75%	62.25%

true label, which is the user’s intended hand gesture, and each row corresponds to the predicted label, which is the gesture actuated by the prosthetic hand.

This equation (4.2) is merely equivalent to the relationship of predictions that the model classified precisely.

$$Accuracy = \frac{\text{The number of correct predictions}}{\text{Total number of predictions}} \quad (4.1)$$

$$= \frac{TP + TN}{TP + TN + FP + FN} \quad (4.2)$$

The average success rate for all subjects without noise was 94.96% on the training set and 91.58% on the test-set. The best-case subject’s training set estimated accuracy was 95.69% and the test set estimated accuracy was 95.50% as shown in Table 2. The impressive point of this experiment was the unique gesture at the last part of the experiment cycle. As the last step of the experiment, users were allowed to demonstrate any kind of creative unique gesture such as crossed fingers, a V-for-victory sign, a finger gun, or the sign of the horns. The prosthetic hand successfully captured these gestures with a high percentage (94%).

When measuring EMG sensors, sometimes sensor values bounce with subjects’ extreme

actions. This noise makes it difficult to obtain sustainable high-quality electromyography signals for the long term without tightening the sensor on the arm. To record an undisturbed sensor signal, a more elaborate connection apparatus is needed than the prototype model possessed. This would further improve the system's accuracy.

As shown in Fig. 4.5, the average success rates with the features extracted using the RBF kernel SVM classifier **ML1ML2**, exhibit higher accuracy with reduced noise levels.

This result demonstrates that applying user-customized training software into the prosthetic hand can suffice for individual user requirements with high performance.



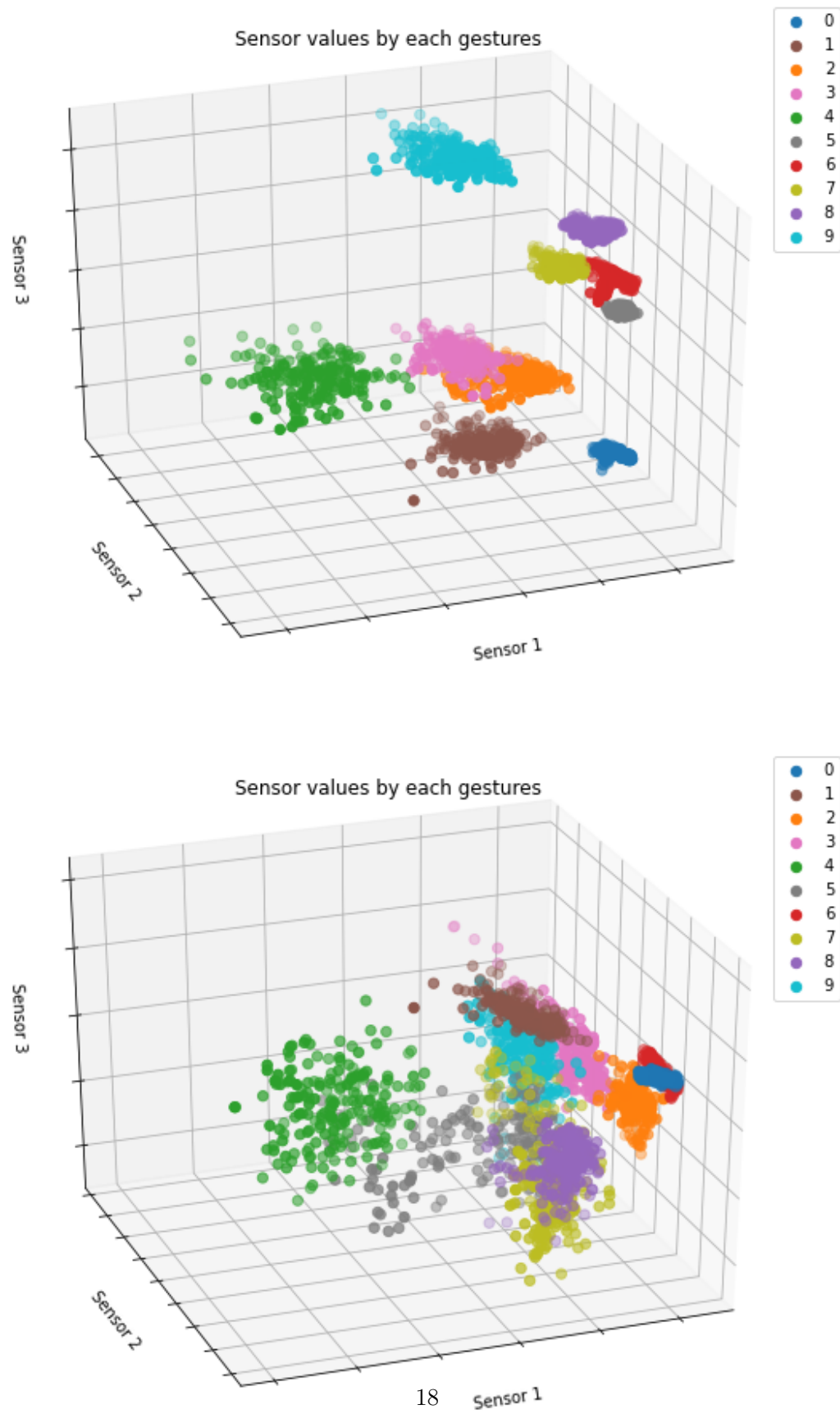


**Figure 4.3** Collected 3-channel EMG sensor values for each different action

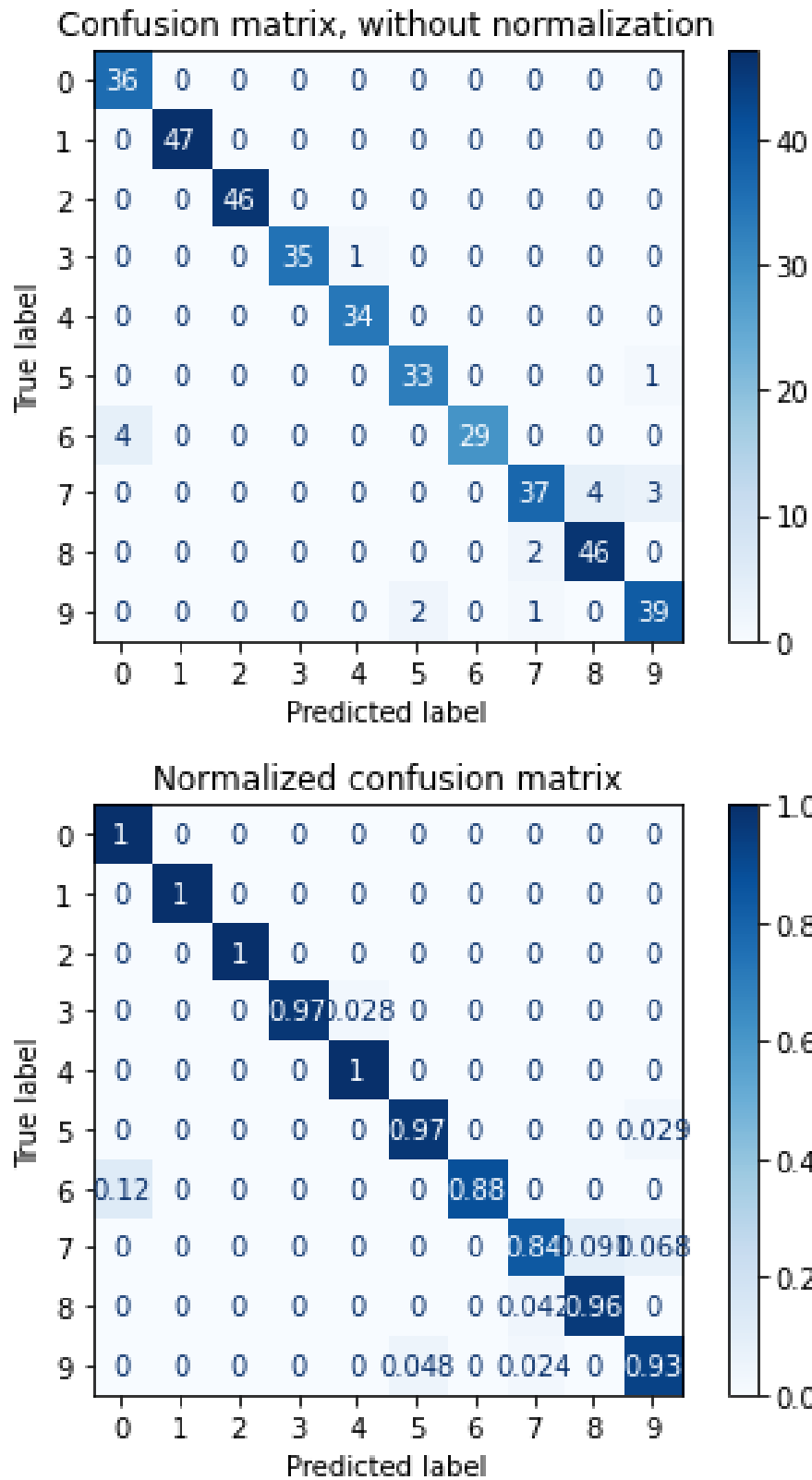
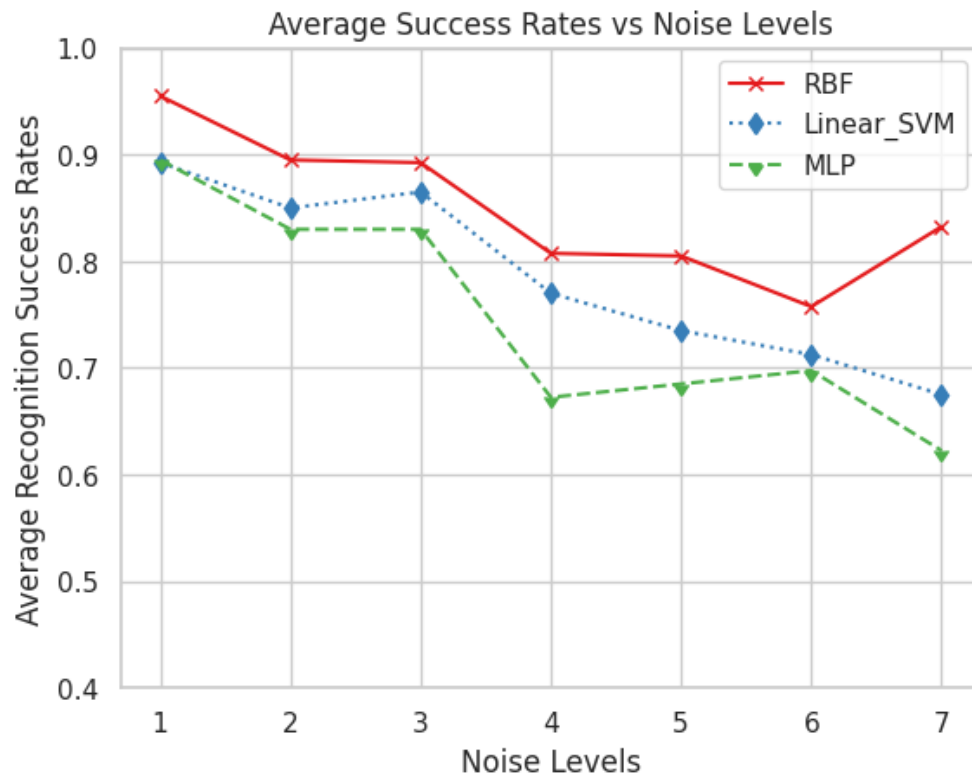


Figure 4.4 Confusion matrix represents the accuracy per user action label



**Figure 4.5** Average recognition success rates of the trained RBF network, linear SVM network, and MLP network under different levels of noise inputs

## CHAPTER V

## CONCLUSION

### 5.1 Self-trainable 3D-printed prosthetic hands

This work demonstrates an architecture that can provide self-trainable actions of sufficient quality to produce a high-performing prosthesis with a low economic cost. We have produced and tested such a control system for a very-low-cost 3D-printed prosthetic hand, and obtained very high performance. Obtaining sustainable high-quality electromyography signals over the long term is still challenging, however. A more elaborately manufactured myography harness than was possible with our prototype is necessary for undisturbed sensor signal recording, which is directly connected to long-term performance at high accuracy. Our future work will focus on embodied EEG-based prosthetic hands control with real amputee subjects' experiments.

### 5.2 Milestone

Self-Trainable 3D-Printed Prosthetic Hands

Oklahoma State University  
Kyungho Nam

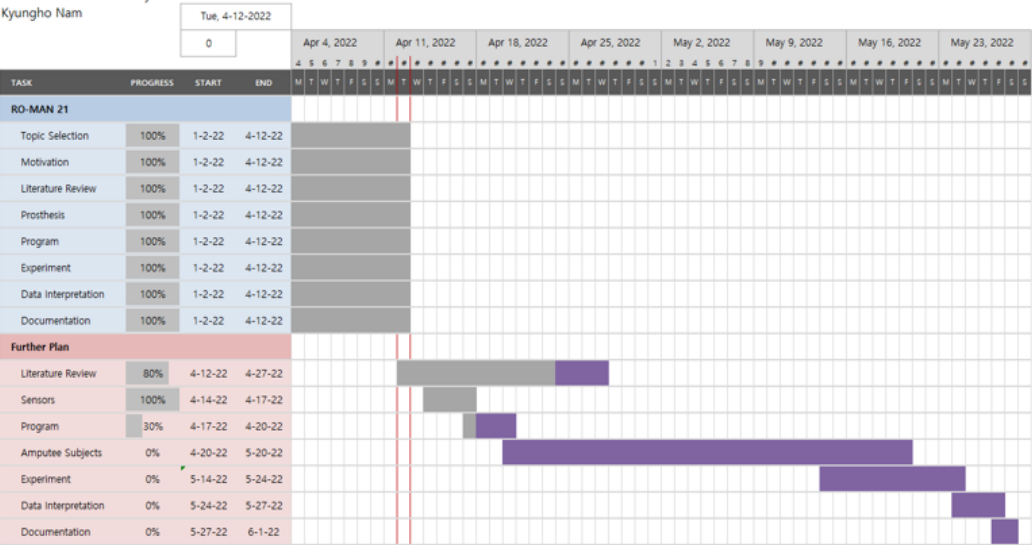


Figure 5.1 Milestone

KYUNGHO NAM

Candidate for the Degree of

Doctor of Philosophy

Thesis: SELF-TRAINABLE 3D-PRINTED PROSTHETIC HANDS

Major Field: Computer Science

Biographical:

Education:

Completed the requirements for the Doctor of Philosophy in Computer Science at Oklahoma State University, Stillwater, Oklahoma in December, 2022.

Completed the requirements for the Bachelor of Science in Electrical Engineering at Oklahoma State University, Stillwater, Oklahoma in December, 2015.